An analytical formalism for the assessment of dose uncertainties due to positioning uncertainties

Wolfgang Lechner[a)] and Dietmar Georg
Division of Medical Physics, Department of Radiation Oncology, Medical University Vienna, 1090 Vienna, Austria

Hugo Palmans
EBG MedAustron GmbH, Marie-Curie Straße 5, 2700, Wiener Neustadt, Austria
National Physical Laboratory, Teddington, TW11 0LW, UK

(Received 20 June 2019; revised 18 December 2019; accepted for publication 18 December 2019; published 26 January 2020)

Purpose: To present an analytical formalism for the in depth assessment of uncertainties of field output factors in small fields related to detector positioning based on dose profile measurements. Additionally, a procedure for the propagation of these uncertainties was developed.
Methods: Based on the assumption that one dimensional and two dimensional second-order polynomial functions can be fitted to dose profiles of small photon beams, equations for the calculation of the expectation value, the variance, and the standard deviation were developed. The following fitting procedures of the dose profiles were considered: A one-dimensional case (1D), a quasi two-dimensional case (2Dq) based on independently measured line profiles and a full 2D case (2Df) which also considers cross-correlations in a two-dimensional dose distribution. A rectangular and a Gaussian probability density function (PDF) characterizing the probability of possible positions of the detector relative to the maximum dose were used. Uncertainty components such as the finite resolution of the scanning water phantom, the reproducibility of the determination of the position of the maximum dose, and the reproducibility of the collimator system were investigated. This formalism was tested in a 0.5 x 0.5 cm^2 photon field where dose profiles were measured using a radiochromic film, a synthetic diamond detector, and an unshielded diode detector. Additionally, the dose distribution measured with the radiochromic film was convoluted with a convolution kernel mimicking the active volume of the unshielded diode.
Results: Analytic expressions for the calculation of uncertainties on field output factors were found for the 1D, the 2Dq, and the 2Df case. The uncertainty of the field output factor related to the relative position of the detector to the maximum dose increased quadratically with increasing limits of possible detector positions. Analysis of the radiochromic film showed that the 2Dq case gave a more conservative assessment of the uncertainty compared to the 2Df case with a difference of $< 0.1\%$. The 2Dq case applied to the film measurements agreed well with the same approach as was applied to the unshielded diode. The investigated uncertainty components propagated to an uncertainty of the field output factors of 0.5% and 0.4% for the synthetic diamond and the unshielded diode, respectively. Additionally, the expectation value was lower than the maximum dose. The difference was 0.4% and 0.3% for the synthetic diamond and the unshielded diode, respectively.
Conclusions: The assessment of uncertainties of field output factors related to detector positioning is feasible using the proposed formalism. The 2Dq case is applicable when using online detectors. Accurate positioning in small fields is essential for accurate dosimetry as its related uncertainty increases quadratically. The observed drop of the expectation value needs to be considered in small field dosimetry. [https://doi.org/10.1002/mp.13991]

Key words: positioning uncertainty, radiation oncology, small field dosimetry

1. INTRODUCTION

Modern radiotherapy treatment techniques such as intensity-modulated radiation therapy (IMRT), volumetric modulated arc therapy (VMAT), and stereotactic radiotherapy utilize small fields for creating a dose distribution optimal for the treatment of the patient. Depending on the size and complexity of the target volume on the one hand and the employed treatment technique, as well as the sequencing algorithms on the other hand, the frequency of small fields compared to the total fluence can vary.[1–5]

Using small fields in radiation oncology requires a state of the art treatment planning system suitable for this task. For beam model creation and commissioning of such a system, special procedures on the determination of field output factors in the small fields need to be considered. In a joint effort, the IAEA and AAPM published a code of practice on small field dosimetry, recommending experimental

procedures as well as detector and field specific correction factors. This code of practice also provides an assessment of the uncertainties of the correction factors themselves.[6,7] These correction factors and the associated uncertainties were based on several publications using experimental[8–16] and Monte Carlo data.[17–22]

Besides the uncertainty of the field output correction factors in small fields, additional uncertainties gain importance. One of these additional contributions to the uncertainty budget is the positioning accuracy of the detector relative to the maximum dose. In small fields, proper alignment is critical, but there are several influencing factors which are beyond control. These include the accuracy of the scanning system, the accuracy of determining the position of the maximum dose and the position of the collimator when repeating measurements.

Bouchard et al performed a Monte Carlo study characterizing the impact of misalignment of the detector relative to the maximum dose. They investigated a maximum displacement of the detector relative to the maximum dose of ± 1 mm assuming a rectangular probability density function (PDF) of the position of the detector.[23] This study shed some light on the magnitude of this type of uncertainty of field output factors. The positioning uncertainty is influenced by the shape of the dose profile which is, amongst other parameters, dependent on the collimator design, on the design of the detector and the assumed maximum displacement of the detector. Therefore, the results presented by Bouchard et al.[23] cannot be generalized to other detector types, beams, or displacement limits of the detector other than used in that study.

In this work, an analytical formalism on determination of uncertainties due to misalignment of a detector relative to the maximum dose based on profile measurements on small fields is presented. Besides the development of the formalism, the main questions addressed in this work were whether the whole two-dimensional beam profile is required or whether two independently measured line profiles are sufficient for a reasonable assessment of positioning uncertainties in small fields. Furthermore, the propagation of this type of uncertainty was explored.

2. MATERIALS AND METHODS

2.A. General formalism

This formalism was developed to assess the contribution of uncertainties related to the position of the detector with respect to the maximum dose, calculated as the relative standard deviation $\sigma_{rel}(D(x,y))$, to the combined standard uncertainty of field output factor measurements. It is considered a type B uncertainty of a single measurement of the maximum dose. The approach follows the recommendations and concepts of the JCGM.[24] Based on the assumption that the dose profile $D(x,y)$ of a small field near the maximum dose can be described using a second-order polynomial function and a given PDF of the detector position relative to the maximum dose $g(x,y)$, the expectation value $E(D(x,y))$, the variance $Var(D(x,y))$, and the relative standard deviation $\sigma_{rel}(D(x,y))$ of the dose measured by the detector can be expressed as follows:

$$E(D(x,y)) = \int_{-\infty}^{\infty}\int_{-\infty}^{\infty} D(x+x_0, y+y_0)g(x,y)dxdy \quad (1)$$

$$Var(D(x,y)) = E\left(D(x,y)^2\right) - E(D(x,y))^2 \quad (2)$$

$$\sigma_{rel}(D(x,y)) = \frac{\sqrt{Var(D(x,y))}}{E(D(x,y))} \quad (3)$$

where x_0 and y_0 are the positions of the maximum of the polynomial used for fitting the dose profiles. Note that for one-dimensional problems only one-dimensional functions and integrals were investigated. For better readability only the formulas for calculating the expectation value and the variance are shown. With these, the relative standard deviation was calculated using Eq. (3) shown in Table V, Figs. 2 and 3.

Solutions of these formulas were used for calculating the contribution to the uncertainty of the dose due to detector positioning. Three different cases were investigated further.

A simple one dimensional dose distribution, described as

$$D(x) = p_{00} + p_{10}x + p_{20}x^2 \quad (4)$$

A quasi two-dimensional dose distribution, where two independent polynomial functions were fitted to two independent dose profiles in x and y direction, expressed as follows:

$$D(x) = p_{00} + p_{10}x + p_{20}x^2 \quad (5)$$

$$D(y) = p_{00} + p_{01}y + p_{02}y^2 \quad (6)$$

The two-dimensional (2D) second-order polynomial function

$$D(x,y) = p_{00} + p_{10}x + p_{20}x^2 + p_{01}y + p_{02}y^2 + p_{11}xy \quad (7)$$

was fitted to a two-dimensional dose distribution and is henceforth referred to as full 2D dose distribution. The resulting expressions from the application of Eqs. (1), (2) and (3) to the different fits describing the respective dose distributions are summarized in Table I for different PDFs. A graphical representation of the fitted dose profile and a rectangular as well as a Gaussian PDF are shown in Fig. 1. Mathematical details on the approach and an example on the calculation of this type of uncertainty can be found in the Supporting information.

2.B. Uncertainty propagation

As the dose distribution around the maximum dose is not linear, conventional Gaussian uncertainty propagation is not applicable. To investigate the propagation of uncertainties, various convolutions of rectangular and Gaussian PDFs were performed and the resulting PDFs were applied to the formalism

TABLE I. A summary of expressions for the calculation of the expectation value and the variance for the assessment uncertainties of point dose measurements due to the relative displacement of the detector with respect to the maximum dose. Two different probability density functions (PDFs), a rectangular and a Gaussian, were applied to the one dimensional, quasi two dimensional and full two dimensional dose distribution. The parameters a and b are the half width of the rectangular PDF and the parameters s_x and s_y are the standard deviation of the Gaussian PDF in x and y direction, respectively.

	Probability density function			
Dose distribution	Rectangular		Gaussian	
1D				
$g(x)$	$\frac{1}{2a}$	(8)	$\frac{1}{\sqrt{2\pi s_x^2}} e^{-\frac{x^2}{2s_x^2}}$	(17)
$E(D(x))$	$p_{00} - \frac{p_{10}^2}{4p_{20}} + \frac{a^2 p_{20}}{3}$	(9)	$p_{00} - \frac{p_{10}^2}{4p_{20}} + s_x^2 p_{20}$	(18)
$Var(D(x))$	$\frac{4a^4 p_{20}^2}{45}$	(10)	$2s_x^4 p_{20}^2$	(19)
Quasi 2D				
$g(x); g(y)$	$\frac{1}{2a}; \frac{1}{2b}$	(11)	$\frac{1}{\sqrt{2\pi s_x^2}} e^{-\frac{x^2}{2s_x^2}}; \frac{1}{\sqrt{2\pi s_y^2}} e^{-\frac{y^2}{2s_y^2}}$	(20)
$E(D(x)); E(D(y))$	$p_{00} - \frac{p_{10}^2}{4p_{20}} + \frac{a^2 p_{20}}{3}; p_{00} - \frac{p_{01}^2}{4p_{02}} + \frac{b^2 p_{02}}{3}$	(12)	$p_{00} - \frac{p_{10}^2}{4p_{20}} + s_x^2 p_{20}; p_{00} - \frac{p_{01}^2}{4p_{02}} + s_y^2 p_{02}$	(21)
$Var(D(x)); Var(D(y))$	$\frac{4a^4 p_{20}^2}{45}; \frac{4b^4 p_{02}^2}{45}$	(13)	$2s_x^4 p_{20}^2; 2s_y^4 p_{02}^2$	(22)
Full 2D				
$g(x,y)$	$\frac{1}{4ab}$	(14)	$\frac{1}{2\pi s_x s_y} e^{-\frac{1}{2}\left(\frac{x^2}{s_x^2}+\frac{y^2}{s_y^2}\right)}$	(23)
$E(D(x,y))$	$\frac{a^2 p_{20} + b^2 p_{02}}{3} + C$	(15)	$s_x^2 p_{20} + s_y^2 p_{02} + C$	(24)
$Var(D(x,y))$	$\frac{4a^4 p_{20}^2 + 5a^2 b^2 p_{11}^2 + 4b^4 p_{02}^2}{45}$	(16)	$2s_x^4 p_{20}^2 + s_x^2 s_y^2 p_{11}^2 + 2s_y^4 p_{02}^2$	(25)
C	$\frac{p_{02} p_{10}^2 - p_{01} p_{10} p_{11} + p_{00} p_{11}^2 + p_{01}^2 p_{20} - 4 p_{00} p_{02} p_{20}}{p_{11}^2 - 4 p_{02} p_{20}}$	(26)		

described in Eqs. (1) and (2). The resulting equations for the one dimensional case are summarized in Tables II and III.

2.C. Experimental data

All measurements were performed in a 6 MV photon beam produced by a Versa HD (Elekta AB, Stockholm, Sweden) equipped with an Agility multi-leaf collimator (MLC) with 5 mm isocentric leaf width. The investigated nominal field size was 0.5 cm x 0.5 cm. All measurements were performed using an SSD of 90 cm and a depth of 10 cm water. The 2D dose distribution was determined using Gafchromic EBT3 films (Ashland Advanced Materials, Bridgewater, NJ, USA) in a solid water phantom (Gammex/Sun Nuclear Corporation, Melbourne, Australia). The film was scanned using an Epson V700 scanner (Epson, Nagano, Japan) 24 h after irradiation.[25,26] The resulting dose distribution was convolved with a disc-shaped convolution kernel with 1.2 mm diameter to mimic the active volume of a PTW 60017 DiodeE detector (PTW, Freiburg, Germany). For testing the full 2D approach, the parameters of Eq. (7) were fitted to a 2.4 mm x 2.4 mm area around the maximum dose. Line profiles in x and y

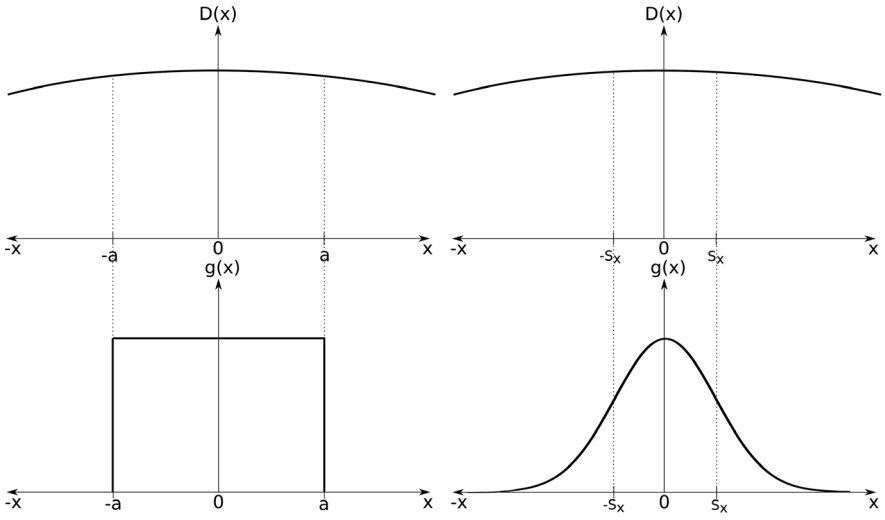

FIG. 1. Example of a one dimensional profile. On the left, the probability of the detector position with respect to the maximum dose is assumed to be equal within the limits $-a$ and a. On the right, the probability of the detector position with respect to the maximum dose is assumed to follow a Gaussian distribution with the standard deviation s_x.

TABLE II. Formulas for the expectation value using various combinations of probability density functions (PDFs): Eq. (27) two rectangular PDFs, Eq. (28) a Gaussian and a rectangular PDF, Eq. (29) a rectangular and a Gaussian PDF and Eq. (30) two Gaussian PDFs. The parameters a and b are the half width of the rectangular PDF and the parameters s_x and s_y are the standard deviation of the Gaussian PDF in x and y direction, respectively.

$\boldsymbol{E(D(x))}$	Rectangular $\boldsymbol{a_1}$	Gaussian $\boldsymbol{s_1}$
Rectangular $\boldsymbol{a_2}$	$p_{00} - \frac{p_{10}^2}{4p_{20}} + p_{20}\left(\frac{a_1^2}{3} + \frac{a_2^2}{3}\right)$ (27)	$p_{00} - \frac{p_{10}^2}{4p_{20}} + p_{20}\left(s_1^2 + \frac{a_2^2}{3}\right)$ (28)
Gaussian $\boldsymbol{s_2}$	$p_{00} - \frac{p_{10}^2}{4p_{20}} + p_{20}\left(\frac{a_1^2}{3} + s_2^2\right)$ (29)	$p_{00} - \frac{p_{10}^2}{4p_{20}} + p_{20}\left(s_1^2 + s_2^2\right)$ (30)

TABLE III. Formulas for the variance using various combinations of probability density functions (PDFs): Eq. (31) two rectangular PDFs, Eq. (32) a Gaussian and a rectangular PDF, Eq. (33) a rectangular and a Gaussian PDF and Eq. (34) two Gaussian PDFs. The parameters a and b are the half width of the rectangular PDF and the parameters s_x and s_y are the standard deviation of the Gaussian PDF in x and y direction, respectively.

$\boldsymbol{Var(D(x))}$	Rectangular $\boldsymbol{a_1}$	Gaussian $\boldsymbol{s_1}$
Rectangular $\boldsymbol{a_2}$	$p_{20}^2 \frac{4a_1^4+20a_1^2a_2^2+4a_2^4}{45}$ (31)	$p_{20}^2\left(2s_1^4 + \frac{4}{3}s_1^2a_2^2 + \frac{4a_2^4}{45}\right)$ (32)
Gaussian $\boldsymbol{s_2}$	$p_{20}^2\left(\frac{4a_1^4}{45} + \frac{4}{3}s_2^2a_1^2 + 2s_2^4\right)$ (33)	$2p_{20}^2\left(s_1^2 + s_2^2\right)^2$ (34)

direction were also extracted and Eqs. (5) and (6) were fitted to the respective line profiles.

To assess the differences between the full 2D approach and the quasi 2D approach using two independent one-dimensional (1D) profiles in clinically realistic scenarios, both methods were executed and compared. One-dimensional profiles in the x an y direction were acquired using a PTW 60019 microDiamond and a PTW 60017 DiodeE in a PTW MP3 water phantom. The microDiamond is a synthetic diamond detector. The active volume has a diameter 2.2 mm and a thickness of 1 µm. The DiodeE is a p-type silicon diode with a diameter of 1.2 mm and a thickness of 30 µm. A step size of 0.1 mm was used for profile scanning using the online detectors. The resulting assessments of uncertainty of the DiodeE detector were compared to the film measurements mimicking measurements using the DiodeE. This allowed a comparison of uncertainties derived using a full two dimensional dose distribution with uncertainties derived from two independent line profiles. Additionally, other sources of uncertainties related to the relative position of the DiodeE to the maximum dose were investigated. The reproducibility of finding the position of the maximum dose was assessed by repeated acquisition of five dose profiles without switching the beam off between measurements, thereby keeping the MLCs and jaws fixed. The reproducibility of the position of maximum dose itself when changing the field geometry was assessed by repeated measurements of dose profiles. For these measurements the field size was set to 10 x 10 cm^2 and reset to the 0.5 x 0.5 cm^2 field between measurements. This process was repeated five times in one measurement session.

3. RESULTS

The results of the fitting procedures for the different dose distributions are summarized in Table IV. As depicted in Figs. 2 and 3, with increasing limits of the detector displacement a of the rectangular PDF or the standard deviation of the Gaussian PDF s_x also σ_{rel} increased following a quadratic function. The examples presented in Table V represent prototypes of uncertainty contributions encountered in small fields due to positioning of the detector with a rectangular PDF. A limit of detector displacement a of 0.05, 0.25, and 1 mm correspond to the accuracy of a state of the art scanning water phantom, a previous generation scanning water phantom and the uncertainty of the room lasers, respectively.

The aspect of a lower expectation value than the maximum dose is shown in Figs. 4 and 5. The expectation value with respect to the maximum of the dose distribution is shown as a function of the investigated limit of detector displacement for the rectangular PDF and standard deviation of the Gaussian PDF. This ratio decreased following a quadratic function with increasing limits of detector displacement or standard deviation. This drop of the expectation value was larger than 1% for $a > 0.5$ mm for the rectangular PDF and for $s_x > 0.3$ mm for the Gaussian PDF.

TABLE IV. Fitting parameters of the film measurements considering the full two-dimensional dose distribution, the film measurements of using two independent one-dimnesional (1D) dose distributions, two independent 1D dose distributions acquired with the DiodeE as well as the microDiamond.

Detector	Function	p_{00}	p_{10}	p_{20}	p_{01}	p_{02}	p_{11}
Film	$D(x,y)$	225.6	−1.494	−14.32	−0.2671	−11.94	0.2027
Film	$D(x)$, $D(y)$	225.0	−1.106	−15.09	0.0071	−12.76	0
DiodeE	$D(x)$, $D(y)$	1.002	−0.0183	−0.0611	−0.0129	−0.0631	0
microDiamond	$D(x)$, $D(y)$	0.998	−0.0020	−0.0582	−0.0012	−0.0747	0

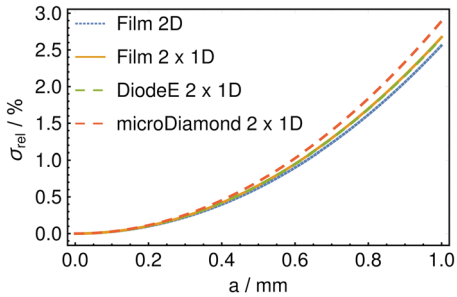

FIG. 2. Relative standard deviation of the dose as a function of a. A two-dimensional rectangular probability density function with symmetric limits ($a = b$) was used for this calculation. [Color figure can be viewed at wileyonlinelibrary.com]

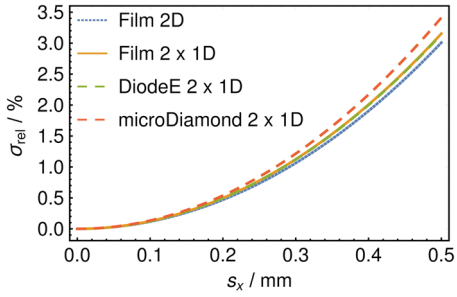

FIG. 3. Relative standard deviation of the dose as a function of s_x. A two-dimensional Gaussian probability density function with symmetric standard deviations ($s_y = s_x$) was used for this calculation. [Color figure can be viewed at wileyonlinelibrary.com]

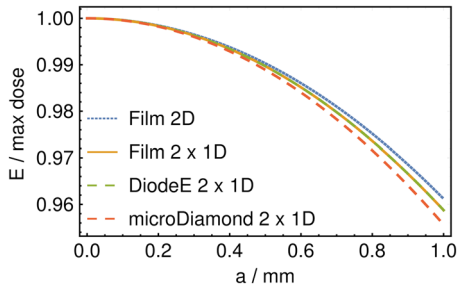

FIG. 4. Expectation value of the dose with respect to the maximum dose as a function of a. A two-dimensional rectangular probability density function with symmetric limits ($a = b$) was used for this calculation. [Color figure can be viewed at wileyonlinelibrary.com]

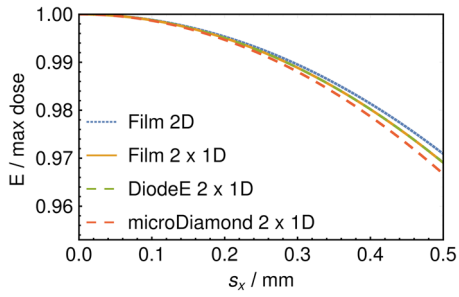

FIG. 5. Expectation value of the dose with respect to the maximum dose as a function of s_x. A two-dimensional Gaussian probability density function with symmetric standard deviations ($s_y = s_x$) was used for this calculation. [Color figure can be viewed at wileyonlinelibrary.com]

The standard uncertainty and the drop of the expectation value derived using the two line profiles, which were fitted independently to the 2D dose measured using film, agreed well with those derived using the DiodeE. A direct comparison σ_{rel} for the two investigated detectors showed a slightly larger uncertainty for the microDiamond having a larger active volume compared to the DiodeE.

Acquiring five profiles without changing the field geometry between the measurements showed a standard deviation of the position of the maximum dose relative to the detector position of 0.05 and 0.01 mm in x and y direction, respectively. Acquiring five profiles with changing the field size between the measurements revealed a standard deviation of the position of the maximum dose relative to the detector position of 0.04 and 0.22 mm in x and y direction, respectively. The square sum of these two contributions to the positioning uncertainty were 0.06 and 0.22 mm for s_x and s_y, respectively. The scanner resolution of the water phantom was isotropic 0.1 mm, as stated by the manufacturer. Therefore, a is equal to b with 0.05 mm. In this example, the total uncertainty was based on an uncertainty contribution with an underlying rectangular and a Gaussian PDF. These uncertainties propagated according to Eqs. (28) and Eq. (32) or Eqs. (29) and (33) in Tables II and III to a combined relative standard uncertainty related to the detector position of 0.5% for the microDiamond and 0.4% for the DiodeE. The ratio of the expectation value to the maximum dose was 0.996 and 0.997 for the microDiamond and the DiodeE, respectively.

TABLE V. Relative standard deviation of the dose for selected limits of detector displacement. For these examples a symmetric limit of detector displacement ($a = b$) was used.

σ_{rel}/%		a/mm			
Detector	Function	0.05	0.25	0.5	1
Film	$D(x,y)$	<0.1	0.15	0.6	2.6
Film	$D(x), D(y)$	<0.1	0.16	0.7	2.6
DiodeE	$D(x), D(y)$	<0.1	0.16	0.7	2.7
microDiamond	$D(x), D(y)$	<0.1	0.18	0.7	2.9

4. DISCUSSION

In this work an analytical formalism for the assessment of uncertainties of field output factors due to positioning uncertainties in small fields was introduced. The uncertainty of 2.7% (shown in Table V) derived for the DiodeE using a rectangular PDF with a half-width of 1 mm was comparable to the value of 3.3% published by Bouchard et al. for the same type of detector.[23] It needs to be mentioned that the 0.5 x 0.5 cm^2 field used in this work had an equivalent square field size, as defined in TRS-483,[6] of 0.56 cm. With clinically realistic spatial uncertainties the relative standard deviation was 0.5% and 0.4% for the microDiamond and the

DiodeE, respectively. For these examples, the uncertainty contribution related to positioning is approximately half the uncertainty of the field output correction factor of 0.8% as stated in TRS-483 for these types of detectors and that particular field size.[27] Additionally, the uncertainty of determining the field size itself is a major contributor to the total uncertainty of field output factor measurements. The reason for that is the high sensitivity of the field output factor with respect to small field sizes. This sensitivity can be in the order of 20%/mm for an 0.5 cm × 0.5 cm field. Assuming an uncertainty of only 0.1 mm of determining the field size would already cause an uncertainty related to the determination of the field size of 2%.

For field sizes of 1 cm x 1 cm and larger, the positioning uncertainty becomes negligible for the investigated detectors (results not shown). A re-assessment of the field size dependence of the positioning uncertainty needs to be conducted for other detectors, especially for detector with larger active volumes.

A comparison of Eq. (13) with Eq. (16) and Eq. (22) with Eq. (25) in Table I shows that the only difference between the variance of two independent profiles and the full 2D expression is the term containing the parameter characterizing the cross-correlation p_{11}. Assuming all other parameters of the full 2D dose distribution are the same as of the quasi 2D dose distribution would mean that the variance of the full 2D distribution is always larger than the variance of the quasi 2D distribution using two independent 1D dose profiles. However, with parameters derived from the same EBT3 film shown in Table I, the variance of the quasi 2D dose distributions was actually higher compared to the variance of the full 2D dose distributions. This effect was the same for the rectangular and the Gaussian PDF. Therefore, the quasi 2D approach overestimates the uncertainties compared to the full 2D approach. This might be partially caused by the fitting procedure itself. Fitting the two 1D 2nd polynomials gave a slightly larger curvature than fitting the 2D second-order polynomial to the dose distribution. Field output measurements using online detectors require the measurement of dose profiles before the actual field output factor measurement can be conducted. These dose profiles can be used as input for the proposed quasi 2D approach and give a reasonable assessment of the uncertainties due to the relative position of the detector to the maximum dose. The slightly larger uncertainty of the microDiamond detector compared to the DiodeE might be related to the differences in the size of the active volume. This difference could also be caused by a slight change in collimator positions between measurements with the microDiamond and the DiodeE. Further investigations with a fixed collimator such as stereotactic cones are necessary. For detectors with larger volumes compared to solid state detectors, such as small ionization chambers, an increase of the uncertainty related to positioning of the detector is expected. Using this formalism, the detector and field specific uncertainties related to positioning can be calculated for any detector.

The correct choice of the PDF for the particular uncertainty contribution is essential. For this work, the value of interest was the maximum dose. If the maximum dose is believed to be within a certain interval with no further information on the probability distribution of possible positions, the rectangular PDF will give the most conservative assessment. This is the case for a scanning water phantom which can drive to discrete positions only. For assessing the uncertainty related to the collimation system, repeated measurements were performed. For that type of uncertainty, a Gaussian PDF is the appropriate choice. Equally as important as the correct choice of the PDF for describing a particular uncertainty component, is the selection of the correct set of equations when propagating uncertainties. This work revealed that conventional propagation of uncertainties cannot be applied to uncertainties related to positioning uncertainties of a detector in small fields. When propagating an uncertainty component with a rectangular PDF and an uncertainty component with a Gaussian PDF, Eqs. (28) and Eq. (32) or (29) and (33) in Tables II and III need to be used, as additional terms would be missed if conventional propagation of uncertainties were used. Propagating uncertainty components described by Gaussian PDFs only can be done by adding the variances of the PDFs in the position domain and then calculating the dosimetric uncertainty using the proposed formulas as shown in Eqs. (30) and (34) in Tables II and III. Other types or combinations of PDFs were not investigated in this work.

The development of the uncertainty due to positioning as a function of possible detector displacements highlights the importance of accurate detector and collimator positioning. A reduction of the spatial uncertainty by half, for example, from 0.5 to 0.25 mm, will reduce the uncertainty of the dose approximately by a factor of four (see Table V).

Another observation of this work was the decrease of the expectation value of the distribution with respect to the maximum dose which is the value of interest when measuring field output factors. The implication of this is that no matter how often these measurements are repeated, the measured field output factors will in the vast majority of cases be lower than the maximum dose. For limits of detector displacement of 0.5 mm for a rectangular PDF or standard deviation of 0.3 mm for a Gaussian PDF, this drop is already 1% and increases to 4% for maximum displacements of 1 mm and a standard deviation of 0.5 mm. The example of the microDiamond detector with clinically realistic spatial uncertainties $s_x = 0.06$ m, $s_y = 0.22$ mm, and $a = b = 0.05$ mm shows that the expectation value would be 0.4% lower than the maximum dose. There are three approaches to encounter this issue. First, following the spirit of the JCGM,[24] the inverse of the ratio of the expectation value to the maximum dose could be used as correction factor applied to the field output measurement. Second, the difference could be included as additional contribution to the uncertainty budget. Third, this difference could be neglected provided that it is sufficiently small. This problem is less pronounced for online detectors. For offline detectors, where accurate positioning is much more challenging, the uncertainty due to detector positioning will be higher. With the increasing use of small fields in radiotherapy the need of auditing these fields also increases. One way to conduct such an audit is to distribute offline

detectors to participating centers and evaluate the results centrally in the auditing institution. Auditing institutions need to consider the uncertainties investigated here when providing audits for field sizes below 1 x 1 cm^2.

For the full 2D approach, the PDFs in x and y direction were assumed to be uncorrelated as strong correlations were not expected. Considering correlations of these two PDFs would result in very complicated expressions which are not useful in clinical practice, but can be used if necessary. No general analytical expressions were found for error propagation for the full 2D approach involving rectangular and Gaussian PDFs. These calculations can be performed numerically.

5. CONCLUSIONS

An analytical formalism for the assessment of uncertainties due to detector position relative to the maximum dose in small fields was presented. The quasi two dimensional case can be used for the assessment of positioning uncertainties in small fields using online detectors. Provided that positioning in small fields is performed according to international guidelines, the uncertainty component of field output factors related to positioning of the detector for fields with an equivalent square field size in the order of 0.6 cm can be kept below 0.5%. Special care in selection of the correct equations must be taken when propagating uncertainty components with different underlying PDFs.

CONFLICT OF INTEREST

The authors have no conflict to disclose.

[a]Author to whom correspondence should be addressed. Electronic mail: wolfgang.lechner@meduniwien.ac.at.

REFERENCES

1. Papp D, Unkelbach J. Direct leaf trajectory optimization for volumetric modulated arc therapy planning with sliding window delivery. *Med Phys*. 2014;41:11701.
2. Craft D, Papp D, Unkelbach J. Plan averaging for multicriteria navigation of sliding window IMRT and VMAT. *Med Phys*. 2014;41:21709.
3. Unkelbach J, Bortfeld T, Craft D, et al. Optimization approaches to volumetric modulated arc therapy planning. *Med Phys*. 2015;42:1367–1377.
4. Gaddy MR, Papp D. Technical note: improving the VMERGE treatment planning algorithm for rotational radiotherapy. *Med Phys*. 2016;43:4093–4097.
5. Lechner W, Primeßnig A, Nenoff L, Wesolowska P, Izewska J, Georg D. The influence of errors in small field dosimetry on the dosimetric accuracy of treatment plans. *Acta Oncol*. 2019:1–7. https://doi.org/10.1080/0284186X.2019.1685127
6. Palmans H, Andreo P, Huq MS, Seuntjens J, Christaki KE, Meghzifene A. *Dosimetry of Small Static Fields Used in External Beam Radiotherapy*. Vienna: International Atomic Energy Agency; 2017. http://www-pub.iaea.org/books/IAEABooks/11075/Dosimetry-of-Small-Static-Fields-Used-in-External-Beam-Radiotherapy
7. Palmans H, Andreo P, Huq MS, Seuntjens J, Christaki KE, Meghzifene A. Dosimetry of small static fields used in external photon beam radiotherapy: summary of TRS-483, the IAEA–AAPM international code of practice for reference and relative dose determination. *Med Phys*. 2018;45:e1123–e1145.
8. Haryanto F, Fippel M, Laub W, Dohm O, Nüsslin F. Investigation of photon beam output factors for conformal radiation therapy–Monte Carlo simulations and measurements. *Phys Med Biol*. 2002;47:N133–N143.
9. Sauer OA, Wilbert J. Measurement of output factors for small photon beams. *Med Phys*. 2007;34:1983–1988.
10. Cranmer-Sargison G, Weston S, Sidhu NP, Thwaites DI. Experimental small field 6 MV output ratio analysis for various diode detector and accelerator combinations. *Radiother Oncol*. 2011;100:429–435.
11. Godwin GA, Simpson JB, Mugabe KV. Characterization of a dynamic multi-leaf collimator for stereotactic radiotherapy applications. *Phys Med Biol*. 2012;57:4643–4654.
12. Ralston A, Liu P, Warrener K, McKenzie D, Suchowerska N. Small field diode correction factors derived using an air core fibre optic scintillation dosimeter and EBT2 film. *Phys Med Biol*. 2012;57:2587–2602.
13. Bassinet C, Huet C, Derreumaux S, et al. Small fields output factors measurements and correction factors determination for several detectors for a CyberKnife(®) and linear accelerators equipped with microMLC and circular cones. *Med Phys*. 2013;40:71725.
14. Lárraga-Gutiérrez JM, Ballesteros-Zebadúa P, , Rodríguez-Ponce M, García-Garduño OA, de la Cruz OOG. Properties of a commercial {PTW}-60019 synthetic diamond detector for the dosimetry of small radiotherapy beams. *Phys Med Biol*. 2015;60:905–924.
15. Tanny S, Sperling N, Parsai EI. Correction factor measurements for multiple detectors used in small field dosimetry on the Varian Edge radiosurgery system. *Med Phys*. 2015;42:5370–5376.
16. Underwood TSA, Rowland BC, Ferrand R, Vieillevigne L. Application of the Exradin W1 scintillator to determine Ediode 60017 and microDiamond 60019 correction factors for relative dosimetry within small MV and FFF fields. *Phys Med Biol*. 2015;60:6669–6683.
17. Francescon P, Cora S, Satariano N. Calculation of k(Q(clin), Q(msr)) (f(clin), f(msr)) for several small detectors and for two linear accelerators using Monte Carlo simulations. *Med Phys*. 2011;38:6513–6527.
18. Cranmer-Sargison G, Weston S, Evans JA, Sidhu NP, Thwaites DI. Implementing a newly proposed Monte Carlo based small field dosimetry formalism for a comprehensive set of diode detectors. *Med Phys*. 2011;38:6592–6602.
19. Czarnecki D, Zink K. Monte Carlo calculated correction factors for diodes and ion chambers in small photon fields. *Phys Med Biol*. 2013;58:2431–2444.
20. Underwood TSA, Winter HC, Hill MA, Fenwick JD. Detector density and small field dosimetry: Integral versus point dose measurement schemes. *Med Phys*. 2013;40:82102.
21. Benmakhlouf H, Sempau J, Andreo P. Output correction factors for nine small field detectors in 6 MV radiation therapy photon beams: a PENELOPE Monte Carlo study. *Med Phys*. 2014;41:41711.
22. Kamio Y, Bouchard H. Correction-less dosimetry of nonstandard photon fields: a new criterion to determine the usability of radiation detectors. *Phys Med Biol*. 2014;59:4973–5002.
23. Bouchard H, Seuntjens J, Kawrakow I. A Monte Carlo method to evaluate the impact of positioning errors on detector response and quality correction factors in nonstandard beams. *Phys Med Biol*. 2011;56:2617–2634.
24. JCGM 100. Evaluation of measurement data — guide to the expression of uncertainty in measurement; 2008.
25. Dreindl R, Georg D, Stock M. Radiochromic film dosimetry: Considerations on precision and accuracy for EBT2 and EBT3 type films. *Z Med Phys*. 2014;24:153–163.
26. Khachonkham S, Dreindl R, Heilemann G, et al. Characteristic of EBT-XD and EBT3 radiochromic film dosimetry for photon and proton beams. *Phys Med Biol*. 2018;63:65007. http://stacks.iop.org/0031-9155/63/i=6/a=065007
27. International Atomic Energy Agency. Dosimetry of small static fields used in external beam radiotherapy. Technical Report Series No. 483. Vienna: International Atomic Energy Agency; 2017. http://www-pub.iaea.org/books/IAEABooks/11075/Dosimetry-of-Small-Static-Fields-Used-in-External-Beam-Radiotherapy

SUPPORTING INFORMATION

Additional supporting information may be found online in the Supporting Information section at the end of the article.

Data S1. Mathematical details on the approach and an example on the calculation of the uncertainty of the maximum dose due to positioning.